

Printing System and Printing Characteristics of Laser Dye Thermal Transfer using a High-Power Laser*

Y. Odai[§], T. Kitamura[†] and H. Kokado[‡]

Graduate School of Science and Technology, Chiba University, 1-33 Yayoicho, Inage-ku, Chiba 263, Japan

M. Katoh

Information Technology R&D Center, Mitsubishi Electric Corp., 5-1-1 Ofuna, Kamakura, Kanagawa 247, Japan

M. Irie[†]

Imaging Systems Lab., Mitsubishi Electric Corp., 1 Babazusho, Nagaokakyo, Kyoto 617, Japan

In laser dye transfer printing, the small laser spot provides high resolution, but the printing speed is relatively low compared to that of thermal head printing, in which a large number of dots can be recorded simultaneously. To shorten the printing time, a compact high-power Nd:YAG laser is used for the light source in our printing system. We have developed a practical laser dye transfer printing system with a newly developed Nd:YAG laser and compact optical head. Printing characteristics with a short pulse, of the order of 1 μ s, are evaluated in this printing system. As a result, continuous-tone printing with a pulse of 2 μ s is feasible when laser power is 1.0 W, indicating a significant advance in printing speeds. The transfer efficiency as a function of pulse width has a peak that can be observed. A thick ink layer produces maximum optical density, although a reduction in efficiency results from increasing the layer thickness. Good halftone printing is also performed using this system.

Journal of Imaging Science and Technology 40: 412–416 (1996)

Introduction

The demand for high-quality, high-speed color printers has been increasing. To respond to this demand, we have been studying ways to increase the printing speed of laser dye transfer.

A laser is used as the heat source instead of a thermal printing head in laser dye transfer printing. Laser absorption material is contained in the ink layer of the ink donor sheet. Very fine dots are produced because only a very small area of the ink is heated by irradiation with the focused laser beam. The significant feature of this printing

method is high resolution, but the printing speed is relatively low if a low-power laser is used. We used a high-power Nd:YAG laser in our printing system to shorten the printing time.

In the past, gas lasers and solid-state lasers such as YAG lasers have been used as heat sources for thermal transfer printing.^{1–3} However, these lasers were not suitable for practical printers because of the large size of the equipment. On the other hand, because semiconductor lasers are now widely used in many industries, these lasers have been used recently in many studies and in commercialization of laser thermal transfer printing.^{4–7} However, the progress in size and performance of solid-state lasers now makes it possible to install these lasers in practical printers. Solid-state lasers have a higher convergence ability than that of high-power semiconductor lasers (~ 300 mW) at present, because they are able to radiate in fundamental mode. Therefore, with solid-state lasers, it is feasible to achieve both high speed and high definition simultaneously.

In this study, we developed a compact Nd:YAG laser that is suitable for the printers, and we miniaturized the optical system. Consequently, we have developed a practical laser dye transfer printing system.⁸ Printing characteristics with a short pulse of several microseconds are examined, using this printing system. Moreover, good halftone images are obtained.

Development of the Printing System

Figure 1 and Table I, show respectively, a schematic diagram and specifications of our printing system. This printing system consists of a laser optical system, a recording drum, and the linear moving mechanism. The printing media are fixed on the aluminum drum, which is 80 mm in diameter and is rotated constantly by the dc motor, using phase-locked loop (PLL) control. The optical head on the linear moving stage is moved at constant pitch by the stepping motor. The moving stage system is composed of a pair of linear guides, a lead screw (pitch is 2 mm), and an aluminum plate.

A Nd:YAG laser device,⁹ 70 mm in length, 10 mm in diameter, and pumped by a high-power laser diode (LD) was fabricated. Maximum output power and wavelength of the Nd:YAG laser are 1.6 W and 1064 nm, respectively. Maximum output power of the pumping LD (SDL-3490-P5, SDL,

Original manuscript received February 15, 1996.

* Presented in part at IS&Ts 11th International Congress on Advances in Non-Impact Printing Technologies, October 29–November 3, 1995, Hilton Head, South Carolina.

† IS&T Member

‡ IS&T Fellow

§ Also affiliated with Information Technology R&D Center, Mitsubishi Electric Corp., 5-1-1 Ofuna, Kamakura, Kanagawa 247, Japan

© 1996, IS&T—The Society for Imaging Science and Technology.

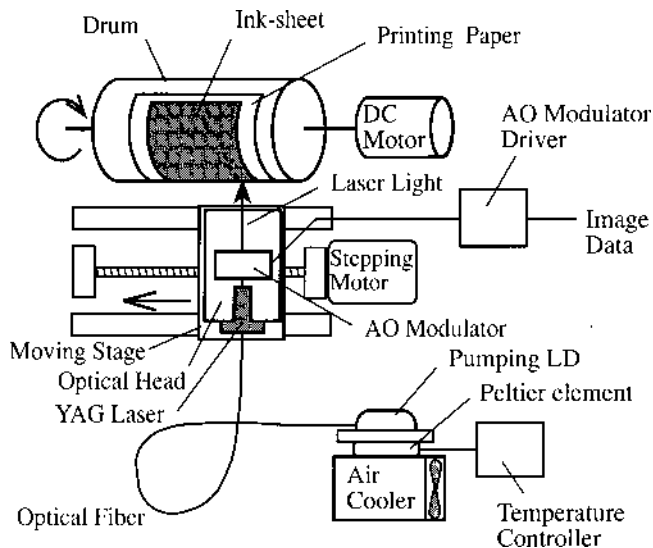


Figure 1. Schematic of the printing system.

TABLE I. Specifications of the Experimental Printing System

Items	Specifications
Resolution (mechanical)	~10,000 dpi
Printing area (max)	200 mm × 300 mm
Printing power	0.1 – 1.1 W
Optical spot diameter (min.)	13 μm
Wavelength of laser	1064 nm
Main scanning velocity	0.13 – 3.18 m/s

TABLE II. Specifications of the Nd:YAG Laser

Items	Specifications
Gain material	Nd: YAG (neodymium: yttrium aluminum garnet)
Dimensions of laser rod	Φ 0.8 mm × 8 mm
Pumping method	LD end-pumping using optical fiber
Output power	1.6 W (continuous wave)
Wavelength	1064 nm
Mode	TEM ₀₀
Beam diameter (1/e ²)	0.45 mm
Beam divergence	3.3 mrad (total angle)
M ² value	< 1.1

Inc.) is 5 W and the wavelength is set at 808 nm to obtain maximum absorption efficiency in the Nd:YAG laser rod. The pumping LD on the air cooler is strictly controlled at constant temperature within 0.1°C, because the wavelength of the LD depends on the temperature. The output light of the pumping LD is led to the end of the Nd:YAG laser through a multimode optical fiber with core diameter 400 μm. The specifications of the Nd:YAG laser are summarized in Table II.

The optical system, which includes the YAG laser, modulator, and converging lens, is set inside the compact optical head, which measures 15 × 10 × 3 cm. The layout of the optical system is shown in Fig. 2. It is possible to miniaturize the optical head more efficiently because the pumping LD unit, which is relatively large, is separated from the optical head. The Z-shaped optical path also contributes to the miniaturization. The overall input/output efficiency of the optical system is 68%, which gives maximum laser power of 1.1 W on the printing medium.

The laser beam from the YAG laser is modulated by an acousto optics (AO) modulator (AOMO 3080-123, Crystal Technology, Inc.). We use the first-order diffracted beam in order to obtain 100% of the on-off ratio. In the AO modula-

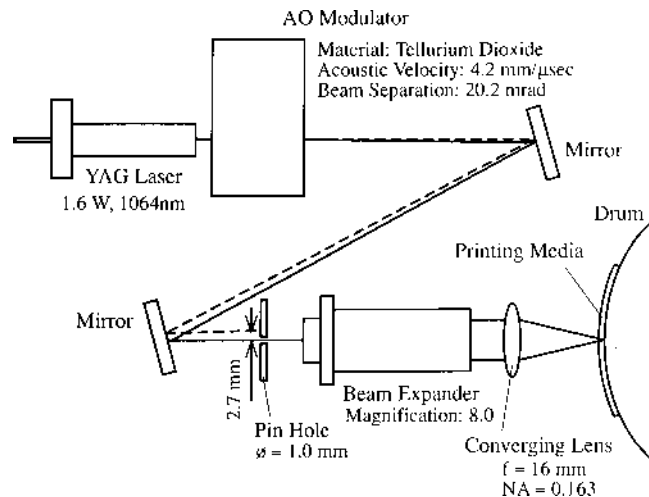


Figure 2. Optical system in the optical head of the printing system.

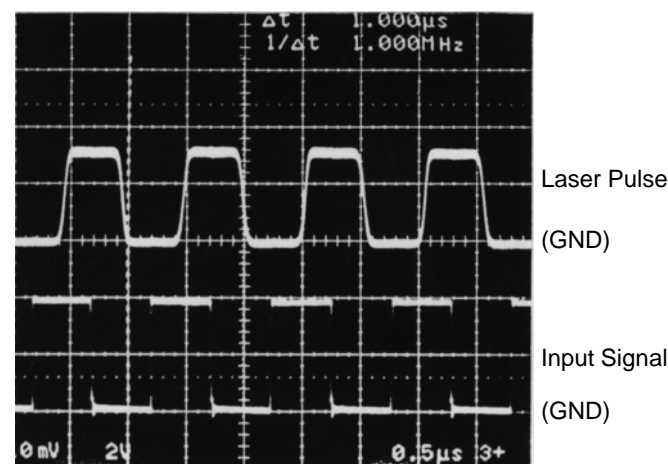


Figure 3. Modulation characteristics.

tor, the risetime t_r increases and the maximum modulation frequency decreases in proportion to the increase of the incident beam diameter d_i as in the following equation¹⁰:

$$t_r = \pi d_i / (2\sqrt{6}V), \quad (1)$$

where acoustic velocity $V = 4.2 \text{ mm}/\mu\text{s}$ for this AO modulator. In contrast, the diffraction efficiency of the AO modulator increases with an increase in the incident beam diameter. Considering the range of modulation frequency used in the experiment, we set the rise time to about 70 ns. Consequently, the incident beam diameter is 0.45 mm, according to Eq. 1. The output beam diameter of the YAG laser is designed to be 0.45 mm, so that direct incidence of the beam into the AO modulator (close arrangement of the AO modulator and the YAG laser) is possible. As a result, the optical system could be simplified and sufficiently miniaturized. Figure 3 shows an evaluation of the modulation characteristics of this optical system. The lower waveform shows a rectangular input signal with frequency 1 MHz and duty 50%, and the upper waveform shows the response signal of the modulated laser beam. We confirmed that satisfactory modulation characteristics were obtained because an almost similar rectangular waveform was reproduced, although a delay time appears.

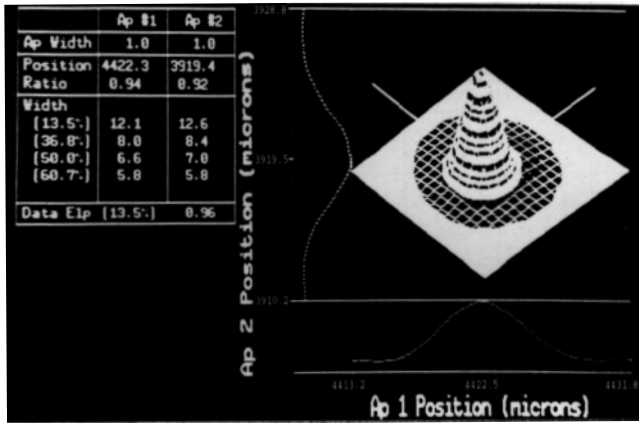


Figure 4. Light intensity distribution of the laser beam on the focal plane, measured by a beam profiling system.

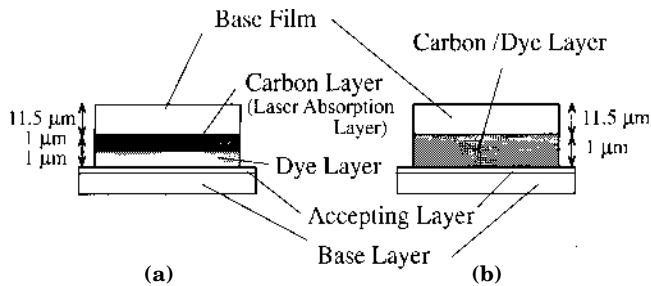


Figure 5. Composition of two types of printing media. (a) Double-layer type and (b) single-layer type.

Next we evaluated the convergence characteristics. The optical spot diameter ($1/e^2$) of the laser beam converged by an idealized optical system can be generally expressed by the following equation:

$$d = 4\lambda f / (\pi D), \quad (2)$$

where wavelength is λ , focal length of the converging lens f , and beam diameter at the lens D . Substituting the actual values of $\lambda = 1064 \text{ nm}$, $f = 16 \text{ mm}$, and $D = 5.2 \text{ mm}$ into Eq. 2 leads to $d = 4.2 \text{ }\mu\text{m}$. Figure 4 shows the light intensity distribution of the laser beam on the focal plane, measured by a beam profiling system (BeamScan Model 2180, Photon, Inc.). The spot diameter was $12.6 \text{ }\mu\text{m}$, which is three times as large as that obtained from Eq. 2. This difference is attributed mainly to aberrations in the optical system because there are many aberration sources, such as the AO modulator, mirrors, beam expander, and lens. However, a good intensity profile, which is nearly Gaussian and isotropic, was obtained.

Experimental

Printing Medium. Figure 5 shows cross-sectional views of printing media for dye sublimation transfer. A double-layer type is shown in Fig. 5(a). The laser absorption layer and the dye layer, each with a thickness of $1 \text{ }\mu\text{m}$, were coated on a transparent base film having a thickness of $11.5 \text{ }\mu\text{m}$. The laser absorption layer is made of polymer in which carbon black is dispersed. The sublimation dye of the ink layer used is the same as that in conventional dye sublimation transfer printing. Figure 5(b) shows a single-layer type. The base film is coated with a color dye mixed with carbon. The printing papers are conventional receiving sheets for video printers.

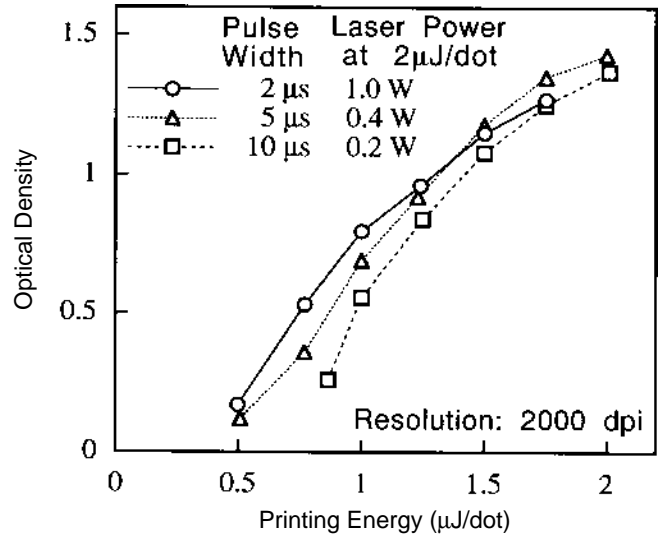


Figure 6. Relationship between optical density and laser power with the variation of pulse width. At the same printing energy, laser power is high when pulse width is small.

In laser dye transfer printing, there are general methods. The first method^{4,5} uses an ink sheet and accepting paper that are separated by a small gap, and the second method¹¹ uses ink sheet and accepting paper that are in direct contact. We used the latter method in this study to minimize experimental parameters.

Printing Energy. Using a single-layer ink sheet, we obtained tone reproduction curves for different pulse width and laser power values. Figure 6 shows the relationship between optical density (OD) and printing energy with pulse widths of 2, 5, and $10 \text{ }\mu\text{s}$. Printing energy was calculated as the product of the laser power and the pulse width. Printing conditions were as follows: resolution 2000 dpi, optical spot diameter $30 \text{ }\mu\text{m}$, and pulse duty 50%. The curves indicate that continuous-tone printing is possible at a pulse of $2 \text{ }\mu\text{s}$ in this system. This figure also reveals that the characteristics of tone reproduction depend slightly on the pulse width. According to the plotted data, with the short pulse width of $2 \text{ }\mu\text{s}$, the OD seems to be saturated earlier in spite of the early rise.

To clarify the characteristics of the tone reproduction, the printing energy per unit area that was required to obtain ODs of 0.5, 1.0, and 1.3 were calculated. Figure 7 shows the relation between printing energy and pulse width with variation of OD. As in Fig. 6, at low OD, 0.5, the printing energy decreases with decreasing pulse width. Low printing energy implies high transfer efficiency. However, the peak of the efficiency shifts toward greater pulse width as OD increases. In summary, reciprocity law failure is observed at both high illuminance and low illuminance in this printing system. The reason the efficiency decreases with greater pulse width is that a part of input energy is lost as heat dissipation. We can explain the decrease of the efficiency at shorter pulse as follows. In the dye diffusion process, OD of printed images generally increases in proportion to the temperature of the ink layer, but OD does not increase when the temperature exceeds a limiting level. When pulse width is very low and laser power is high, the temperature of the ink layer increases drastically and exceeds the limiting level. Consequently, part of the input energy is wasted. If the printing energy is low, the temperature does not reach the limit level even if the pulse is short. Therefore, the decrease of the efficiency at short pulse does not occur.

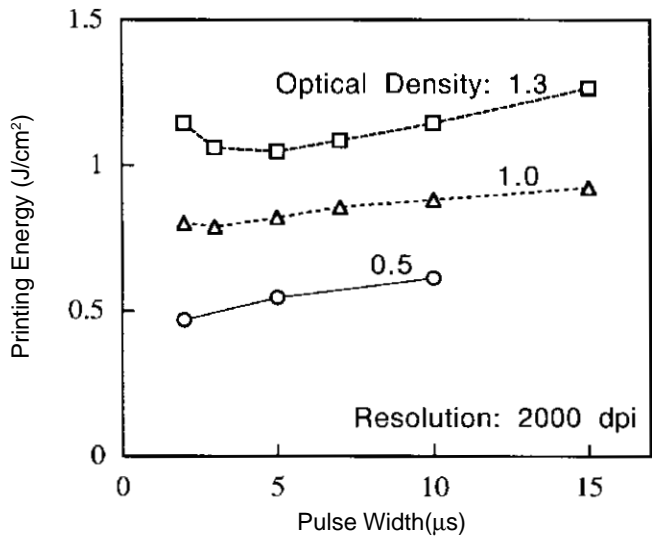


Figure 7. Printing energy per unit area required to obtain the optical density of 0.5, 1.0, and 1.3, as a function of pulse width.

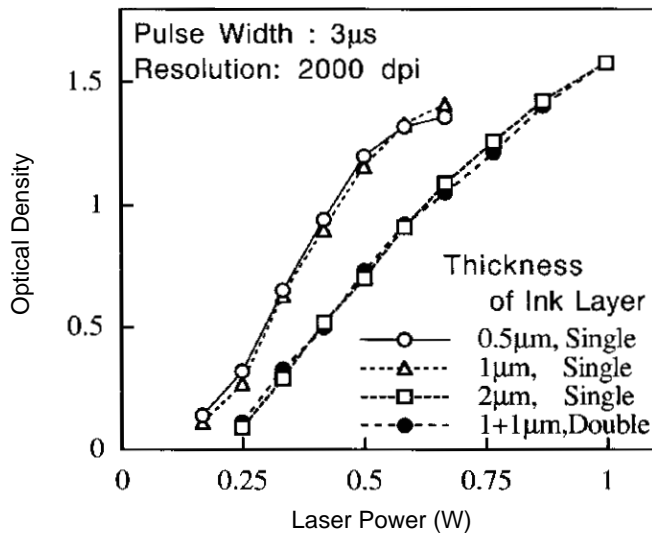


Figure 8. Relationship between optical density and laser power with varied thickness and type of ink layer.

The minimum printing energy per unit area that was required to obtain OD 1.0 was about 0.8 J/cm^2 in this experiment.

Composition and Thickness of the Ink Layer. Figure 8 shows the relationship between OD and laser power with the variation of thickness of the ink layer. For single-layer type, only the thickness of the ink layer was varied; the penetration depth remained the same. The measured light absorptivity at 1064 nm was 92% in the case of the $1 \mu\text{m}$ layer. Figure 8 indicates that the efficiency is low for the $2 \mu\text{m}$ layer. This is due to the large heat capacity of the ink layer. In addition, the maximum value of OD for the $2 \mu\text{m}$ sample is higher than that of the other samples because the thick ink layer contained a larger amount of sublimation dye. On the other hand, the light absorptivity decreases to 72% in the $0.5 \mu\text{m}$ ink layer. Therefore, the effect of small heat capacity is canceled by low light absorptivity. As a result, there is little difference in the efficiency between the $0.5 \mu\text{m}$ and $1 \mu\text{m}$ layer.

When OD was more than about 1.3, not only dye, but also carbon, was transferred to the accepting paper. This carbon transfer occurred for all thicknesses of the single-

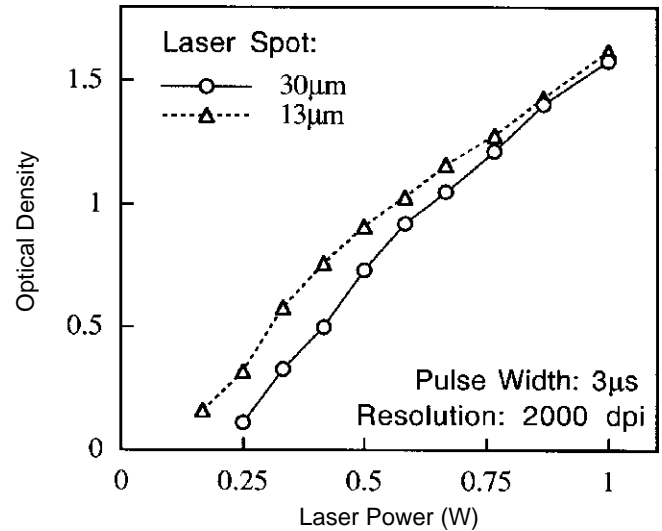


Figure 9. Relationship between optical density and laser power with variations in the optical spot diameter.

layer type. To prevent the carbon transfer, dye and carbon layers were separated in the ink donor sheet. The amount of dye in the ink sheet of the double-layer type is the same as that of the single-layer type with the $2 \mu\text{m}$ ink layer and the light absorptivities of both types being more than 99%. The relation between OD and laser power is also shown in Fig. 8. For the single-layer type and the double-layer type with the same thickness of $2 \mu\text{m}$, almost the same curve is obtained. The reason is that, for the single-layer type, the absorption of the laser light occurs only in the upper half of the ink layer as same as the double-layer type, resulting in temperature distribution nearly equal to that of the double-layer type.

Figure 9 shows the characteristics of tone reproduction for the ink sheet of the double-layer type with varied optical spot diameters. This figure indicates that OD in the case of the smaller, $13 \mu\text{m}$ spot is higher than for the $30 \mu\text{m}$ spot at low laser power but there is little difference in OD in these two cases when high laser power is applied. Therefore, the efficiency with low laser power can be improved by the concentration of the input energy.

Image Printing. Tone reproduction curves in halftone screening were measured. Figure 10 shows the relation between the OD of a gray scale and the input dot area, using the ink sheet of the double-layer type. Printing conditions were as follows: optical spot diameter $13 \mu\text{m}$, pulse width $3 \mu\text{s}$, and laser power 1 W . Halftone conditions (screen 400 lpi; angle of screen 45° ; shape of halftone dot is a circle) were used for the bilevel method. This figure reveals that good tone reproduction is possible, although this characteristic slightly tends to enlarge or increase the contrast of the input data.

Furthermore, we evaluated the high-definition image printing using SCID¹² (standard color image data). SCID (2048×2560 pixels) was converted into bilevel data of the same image size, using the halftone method mentioned above. Figure 11(a) shows the actual size of printed image and Fig. 11(b) a magnified image area. The printing conditions are the same as in the experiment for Fig. 10. Satisfactory halftone image reproduction is obtained, although transferred carbon due to the nonuniformity of the ink sheet is slightly visible in some parts of the image.

Conclusions

A practical laser dye transfer printing system with new developed Nd:YAG laser and compact optical head have

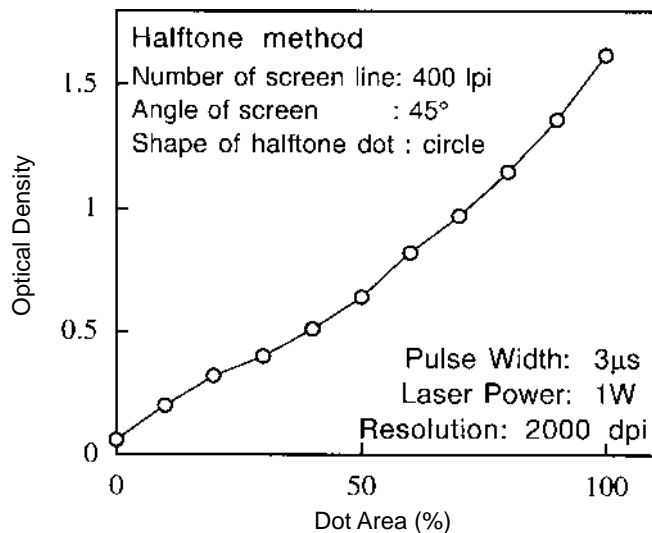


Figure 10. Tone reproduction curve using halftone method.

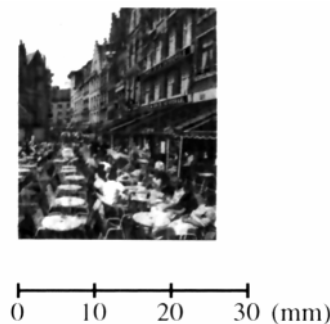
been developed. The maximum printing power is 1.1 W. Good modulation and converging characteristics were confirmed. Printing characteristics with a short pulse of the order of microseconds were evaluated using this printing system. As a result, continuous-tone printing with a short pulse of 2 μ s was feasible when laser power is 1 W, indicating a remarkable advance in printing speed. Reciprocity law failure at both high illuminance and low illuminance were observed. A thick ink layer produced high maximum optical density, although there was a reduction in the efficiency resulting from the increasing of the layer thickness. Moreover, good halftone printing was confirmed using high-definition standard image data.

Optimization of the printing media and a theoretical study are expected to be carried out in future. \blacktriangle

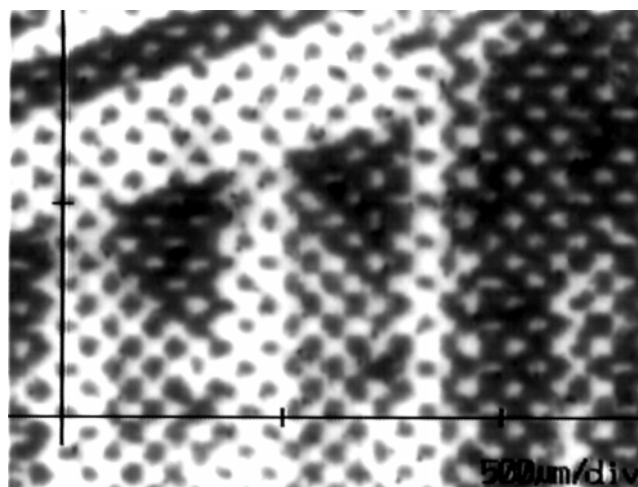
Acknowledgments. The authors express sincere appreciation to K. Tatsumi and Y. Hirano for design and fabrication of the Nd:YAG laser, Dr. K. Kime for design and assembling the optical system. The authors would like to acknowledge the contributions of M. Ohnishi in providing guidelines of this study. The authors also wish to thank T. Takeda and R. Arima for their considerable assistance with the experiment.

References

1. M. L. Levene, R. D. Scott, and B. W. Siry, *Appl. Opt.* **9**: 2260 (1970).
2. C. A. Bruce and J. T. Jacobs, *J. Appl. Photogr. Eng.* **3**: 40 (1977).
3. T. W. Baldock, UK Patent GB2083726A (1982).
4. C. DeBoer, *Proceedings of IS&T's 7th International Congress on Advances in Non-Impact Printing Technologies*, 1991, p. 449.



(a)



(b)

Figure 11. High-definition halftone image samples. (a) Actual size of printed sample and (b) magnified image part.

5. S. Sarraf, C. DeBoer, D. Haas, B. Jadrach, R. Connelly, and J. Kresock, *Proceedings of IS&T's 9th International Congress on Advances in Non-Impact Printing Technologies*, 1993, p. 358.
6. M. Irie and T. Kitamura, *J. Imaging Sci. Technol.* **37**: 231(1993).
7. K. Sumiya, J. Hoshikawa, and A. Kaneko, *Soc. Electrophotogr. Japan* **31**: 524 (1992).
8. Y. Odai, T. Takeda, A. Arima, M. Katoh, T. Kitamura, and H. Kokado, *Proceedings of IS&T's 11th International Congress on Advances in Non-Impact Printing Technologies*, 1995, p. 315.
9. Y. Hirano, K. Tatsumi, and Y. Odai, *Reports on Topical Meeting of the Laser Society of Japan*, No. RTM-94-32, 1994, p. 19.
10. Kwok-leung Yip and E. Muka, *J. Imaging Technol.* **15**: 202 (1989).
11. K. W. Hutt, I. R. Stephenson, H. C. V. Tran, A. Kaneko, and R. A. Hann, *Proceedings of IS&T's 8th International Congress on Advances in Non-Impact Printing Technologies*, 1992, p. 367.
12. The Committee for Standardization of Image Processing Technology, *The Operation Manual of SCID (Standard Color Image Data)*, The Association for Standard of Japan, 1989.